

Epirubicin-calf thymus DNA interaction: a comprehensive investigation using molecular docking, spectroscopy and fluorescent quantum dots

Abbas Hemati Azandaryani¹, Ali Barati², Mohsen Shahlaei³, Mojtaba Shamsipur², Sajad Moradi¹, Elham Arkan^{1*}¹ Nano Drug Delivery Research Center, Kermanshah University of Medical Sciences, Kermanshah, Iran² Faculty of Chemistry, Razi University, Kermanshah, Iran³ Pharmaceutical Sciences Research Center, Kermanshah University of Medical Sciences, Kermanshah, IranCorrespondence to: elhamarkan@yahoo.com, e.arkan@kums.ac.ir

Received March 3, 2018; Accepted May 10, 2018; Published May 30, 2018

Doi: <http://dx.doi.org/10.14715/cmb/2018.64.7.1>

Copyright: © 2018 by the C.M.B. Association. All rights reserved.

Abstract: Reviewing the mode of interaction between this kind of active pharmaceutical ingredients and DNA has received much more attention in current years. Anthracycline drugs such as Epirubicin are frequently used in cancer treatment for breast cancer treatment. In the present study, the Epirubicin -calf thymus DNA interaction was investigated by using spectroscopic, fluorimetric and molecular docking methods. Water-soluble quantum dots (QDs) with nanometric particle size fabricated and characterized by transmission electron microscope and photon correlation spectroscopy. The binding constant value and the free energy change for this interaction were obtained to be $3.00 \times 10^6 \text{ M}^{-1}$ and $-42.26 \text{ kJ mol}^{-1}$, using the spectroscopic method and docking investigations, respectively. Additionally, fluorescent thioglycolic acid-capped CdTe QDs were used for investigation of EPI and DNA interaction. Epirubicin as a quencher quenched the fluorescence of CdTe QDs after electrostatic adsorption on the surface of QDs. With the addition of DNA, EPI will be desorbed from the surface of CdTe QDs, inserted into the DNA. Subsequently, fluorescence changes of QDs were used for calculation of binding constant value, which was in good agreement with that obtained by the spectroscopic method. By the comparison of the achieved results, the intercalation mode of interaction between Epirubicin and DNA proved.

Key words: Epirubicin; DNA interaction; Molecular docking; CdTe QD.

Introduction

Anthracyclines are anticancer complexes that were originally derived from *Streptomyces* bacteria, and their anti-tumor actions were recognized in the 1960s (1). These compounds are used to treat many cancers. Anthracyclines were inhibited the deoxyribonucleic acid (DNA) synthesis by intercalating between base pairs of the DNA strand and also triggers DNA cleavage by topoisomerase II, thus preventing the replication of normal cells and rapidly growing cancer cells (2). Epirubicin (EPI) (Figure 1), as an anthracycline therapeutic agent, is most frequently used in breast cancer treat-

ment. Due to its advantages such as fewer side effects, EPI is more commonly used in cancer treatment. EPI is nowadays commercially accessible for intravenous dosing (3, 4).

DNA is introduced as an important target for cancer therapy. Chemotherapy agents have blocked replication and transcription of DNA in tumor cells with high proliferation rates (5). Thus, DNA is the main target in cancerous cells for chemotherapy drugs, which interact with DNA and suppress the tumor tissue metastasis (6, 7). In this state, the drug with intercalation into the double helix combines with the base pairs and inhibits the replication and synthesis of DNA as well as the ribonucleic acid.

Studying the interactions between biologically active agents and biomolecules (8) could help to understand the structure, nature, and morphology of biomolecules. For a variety of organic, inorganic, and chemical agents present in the environment, the interactions change the secondary structure of DNA. The conformational alterations of DNA, the connection between the molecular structures of the chemical agent, and the mechanisms of DNA interaction have been evaluated in numerous studies (9, 10).

Semiconductor quantum dots (QDs) have frequently investigated for optoelectronic claims (11, 12). QDs stimulated with chemical agents will show the alteration in quenching the photoluminescence property. The modification of QDs causes the variation of electron or energy

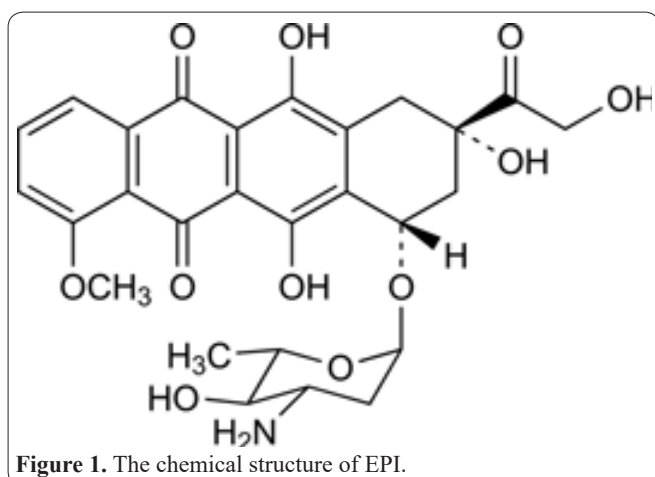


Figure 1. The chemical structure of EPI.

transfer in the donor or receptors of fabricated QDs (13). Some of the photo characteristics of the QDs can be introduced in the molecular diagnosis by altering the concentration signals to optical signals, which can be detected by a simple technique (14). The QDs-fluorescence (FL) resonance energy transfer is one of the photo-based methods which is useful in investigating the biomolecules-small molecule interaction (15), immunoassay, DNA hybridization probe, and enzyme activity measurement (16, 17). At present, many photoinduced electron transfers - based sensors have been applied in detection of a variety of analytes such as glucose, maltose, anion, etc. (18-20). In the photo-induced electron transfer, based on the signal of receptor-substrate, the following mechanism is proposed: firstly, the quencher is adsorbed on the surface of the modified QDs, which quench the QDs FL; in continue, the receptor with high affinity to the quencher is added to the media, which can desorb the quencher by a return in FL of QDs (21).

The objective of this study is an investigation of the interaction between EPI and ct-DNA using spectroscopic, molecular dynamic, and fluorimetric methods and combination of them. The mode of interaction and binding constant (K_b) were obtained by molecular docking (MD) and spectroscopic method. The ability of ct-DNA to separating of EPI from the surfaces of thioglycolic acid-capped CdTe quantum dots (CdTe QDs) investigated in continues. EPI quenches the fluorescence of CdTe QDs by photo-induced electron transfer mechanism.

Materials and Methods

Materials

Tellurium powder, $\text{CdCl}_2 \cdot 5\text{H}_2\text{O}$, NaBH_4 , Epirubicin and Thioglycolic acid (TGA), citric acid, and ethylenediamine were purchased from Sigma-Aldrich (St. Louis, Mo, USA).

Highly polymerized ct-DNA and Tris-HCl were obtained from Sigma Co. For stock solution preparation, the pure ct-DNA was dissolved in Tris buffer with the UV absorbance at 260 and 280 nm >1.8 . The obtained stock was stored at 4 °C and was used for 5 days. The obtained ct-DNA solution was adequately free from impurity. It could be suitable for mentioned working. The concentration of the nucleotide was determined by UV absorption spectroscopy with the $\epsilon=6600 \text{ M}^{-1}\text{cm}^{-1}$ (ϵ : molar absorption coefficient at 260nm).

Apparatus

The particle size of QDs was analyzed using photon correlation spectroscopy (PCS) (Malvern Zetasizer Co, United Kingdom). For this goal, the specific amount of prepared formulation was diluted in ultra-purified water and then the diameter of the suspension was measured. The morphology and size of QDs were evaluated using the transmission electron microscopy (TEM) (JEOL JEM-2000 EX TEM). For this aim, a droplet dispersion of the QDs was thrown down onto a carbon-coated copper grid and was air-dried for particles' size measurement. Absorbance spectra were recorded by an HP spectrophotometer (Agilent 8453).

TGA CdTe QDs preparation procedure

CdTe QDs prepared using several techniques and

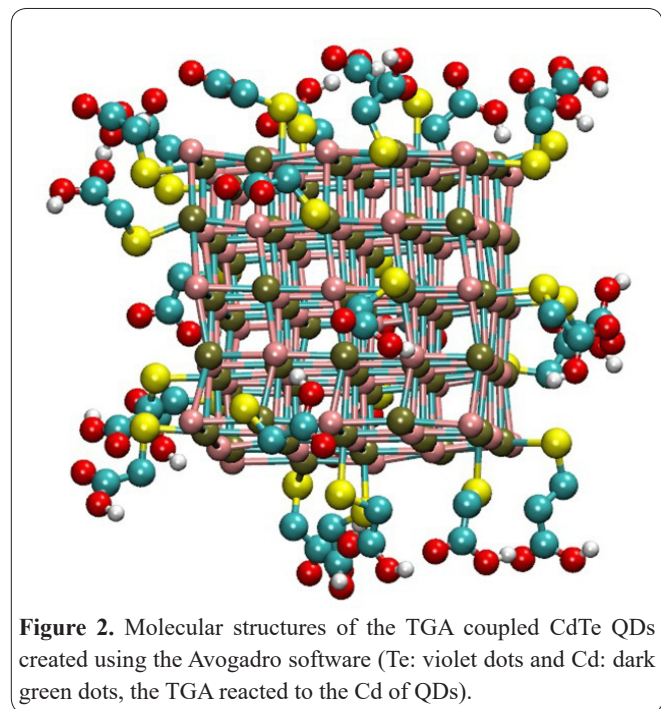
used for several applications (22). In this study, the CdTe QDs were fabricated according to our previously reported study (23). For the QDs preparation, the specified amount of $\text{CdCl}_2 \cdot 5\text{H}_2\text{O}$ (0.5 mmol, 0.137 mg) and TGA (1 mmol, 0.092 mg) were mixed in 100 mL deionized water in a flask to prepare the primary substance of Cd (pH 10 and stirring under N_2 for a half-hour). The 46 mg tellurium powder after reduction with NaBH_4 (40 mg) was converted to NaHTe . NaHTe was transferred to the Cd primary substance of Cd and TGA under stirring. The obtained solution was moved to a stainless steel autoclave at 100 °C for 4 h to achieve the TGA-CdTe QDs. The QDs were stored in dark condition for further studies.

FL study

The CdTe particles were dispersed in distilled water to prepare the stock solution with the $2.0 \times 10^{-3} \text{ mg/mL}$ concentration. After 5 min, the FL at an excitation wavelength of 340 nm was measured. The FL of CdTe QDs measured after EPI addition in the concentrations of 0, 2.0, 4.0, 6.0, 6.0, 10 and 12 $\mu\text{mol L}^{-1}$. A recovery study was carried out on the solutions containing CdTe QDs (0.1 mL), EPI (0.2 mL), and ct-DNA with the concentration between 0–45 mg/L. The DNA was prepared in 5 mL of PBS (20 mM, pH 7.4). The FL measurements were performed after 5 min of DNA addition.

Molecular modeling

Molecular modeling is one of the most important tools used to understand the mechanisms and details of interactions on an atomic scale. The Autodock4 was used to investigate the possibility, and the mode of interaction, as well as differences in the energies of interactions of the EPI with QDS and DNA. Initially, the molecular structures of the EPI and TGA CdTe-QDs (Figure 2) were created using the Avogadro software and energy minimization was done to provide an optimal molecular structure using the steep algorithm. The coordinate file for the natural DNA structure (B DNA (CGCGAATTCGCG)) was obtained from the RCSB



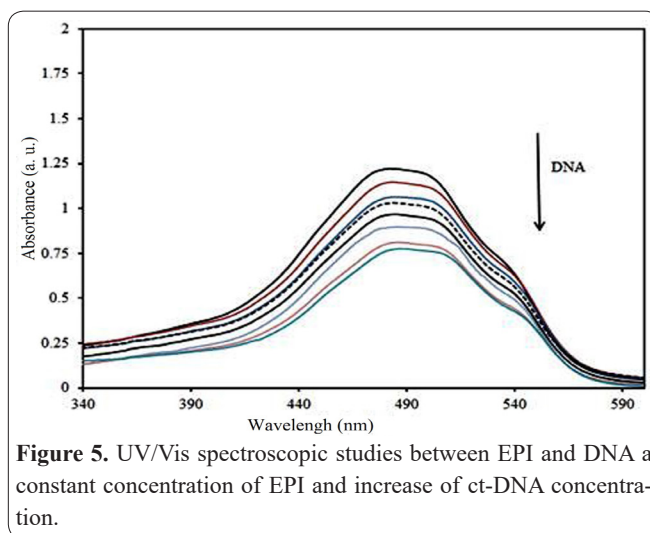
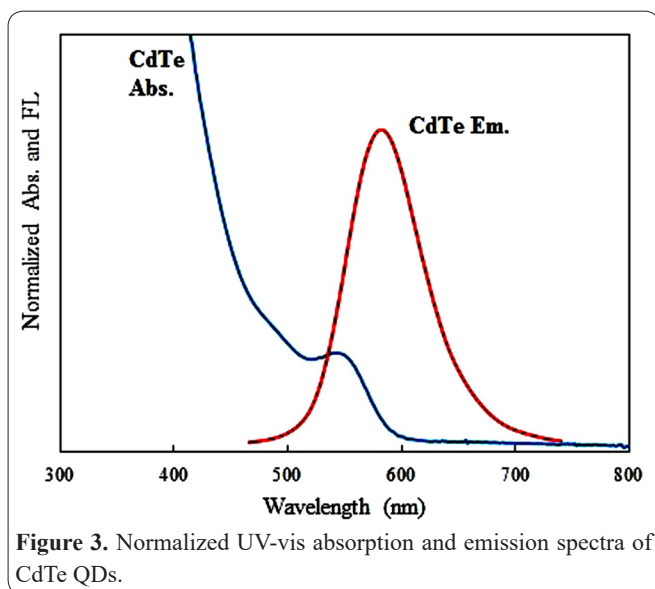


Figure 3. Normalized UV-vis absorption and emission spectra of CdTe QDs.

Figure 5. UV/Vis spectroscopic studies between EPI and DNA a constant concentration of EPI and increase of ct-DNA concentration.

database with the 1BNA code and was used for the docking studies. Adding Gastiger charges and introducing active torsions along with atomic typing of the Autodock force field were done using the MGLtools package. The search space was selected in all calculations so that the ligand would be able to access all parts of the DNA molecule using a box of 82×82×82 points with a grid spacing of 0.375 angstroms. Energetic map types for all involved atom types in all of the phase space were prepared using autogrid4. Eventually, 200 runs under the Lamarck genetic algorithm were calculated for each calculation using autodock4.

Results

Characterization of CdTe QDs

The UV-vis and emission spectra of as-prepared CdTe QDs are shown in Fig. 3. The fabricated modified QDs presented an emission spectrum at nearly 600 nm with the half maximum of about 70 nm. The obtained TGA-CdTe QDs had broad absorption characteristics as shown in Figure 2, which yielded multicolour QDs.

The mean particle sizes of 4.11 ± 1.03 obtained for QDs by PCS investigation as showed in Figure 4 a. A TEM was used to observe morphology and particle size of QDs. From the TEM micrograph as demonstrated in Figure 3 b, the black region shows uniform particle morphology with the diameters nearly around 5 nm.

UV/Vis spectroscopy studies between DNA and EPI

For the spectroscopy study, the concentration of EPI

was kept constant with the value of (5×10⁻⁴ M) and the concentration of ct-DNA varied from 0 to 7.5×10⁻⁴ M (ri [DNA]/[EPI]=0.0–1.5). For the analysis specified amount of aliquots of DNA stock solution were added to the drug solutions and stored in an incubator. Absorbance was recorded at 340 to 600 nm for EPI after the addition of DNA (24).

Figure 5 shows the UV spectroscopy of EPI in the presence of ct-DNA with the maximum absorption 480 nm, and the variation of spectra in the presence of various amounts of ct-DNA was considered. The absorption spectra of EPI and ct-DNA show, when the ct-DNA added to the EPI the spectra decreased with the slight red shift. The absorbance of the EPI decreased upon ct-DNA addition, indicating the interaction between drug and ct-DNA.

Drugs interact with DNA via mainly three different binding modes: intercalation, groove binding, and ionic interactions (25) with K_b numerously were used for this phenomenon survey. To have a better investigation of the kind of interactions, the intrinsic K_b between the chemical agents and nucleotides was calculated using Eq. 2 (26).

$$\frac{[DNA]}{(\epsilon_a - \epsilon_f)} = \frac{[DNA]}{(\epsilon_b - \epsilon_f)} + \frac{1}{K_b(\epsilon_b - \epsilon_f)} \quad \text{Eq. 2}$$

Which in the Eq. 2 [DNA] is the amount of ct-DNA in the nucleotide; ε_b, ε_a, and ε_f are bound to complex, apparent and free extinction coefficients in the equation. The ε_a was calculated as the measured absorbance divided to the EPI concentration before ct-DNA addition. In addition, the ε_f was achieved by a calibration curve of the pure EPI, following Beer's law.

Figure 6 shows the plot of [ct-DNA]/(ε_a - ε_f) versus [ct-DNA]. The slope of this chart is 1/(ε_b - ε_f) and a y-intercept is 1/ K_b (ε_b - ε_f), in which K_b calculated the slope divided to the y-intercept.

The amount of the hypochromism was investigated using Eq. 3 in the 248 nm:

$$H\% = [(A_{Free} - A_{Bounded}) / A_{Free}] \times 100; \quad (1)$$

Generally, the hypochromism has shown the binding strength. The absorption bands of EPI at about 480 nm show hypochromism of 29.9% with the slightly red shift. The obtaining results are the proof that investiga-

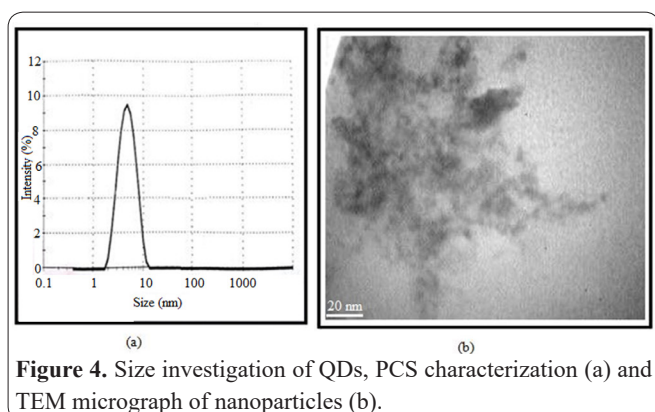


Figure 4. Size investigation of QDs, PCS characterization (a) and TEM micrograph of nanoparticles (b).

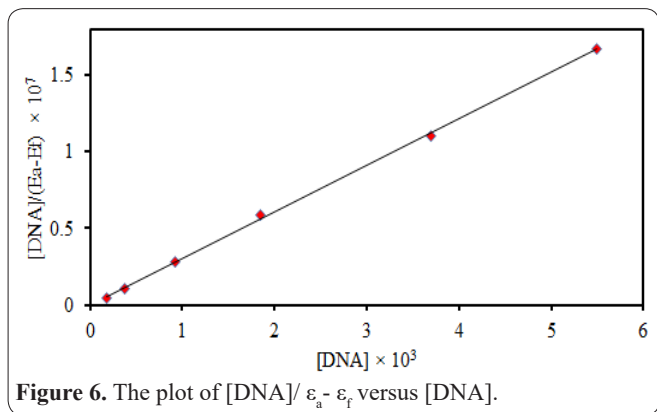


Figure 6. The plot of $[DNA]/\epsilon_a - \epsilon_r$ versus $[DNA]$.

ted agent is inserted into ct-DNA (27).

Molecular docking analysis between EPI and CT-DNA

The possibility and mode of the EPI binding to ct-DNA and TGA capped CdTe-QDs, along with the differences in the energy of these interactions were studied using the Autodock4 software.

Figure 7a and b show that the EPI is capable of interacting with both molecules with acceptable binding energy. It can be predicted that these interactions are stable under the standard conditions. The docking run results are listed in Table 1. Also, EPI was introduced to the A–T (10.8 Å) base pairs compared to G–C (13.2 Å) ones, due to preferential binding of planer aromatic with hydroxyl moiety of EPI to A–T regions rather than G–C parts, which leads to the van der Waals interaction and hydrophilic contacts of the investigated agent and the functional groups of the DNA. The significant result is the lower binding energy of the EPI - DNA compared with EPI – QDs (Table 1). In the solution, ct-DNA can effectively separate the EPI from the quantum dot surface and restore the intensity of the light emitted by QD. These results are in full agreement with the experimental results and confirm the possibility of the switched off-on mechanism of the prepared structure for further applications, for instance in bio-sensing, biomacromolecular structures investigation, and so on.

From the MD study, the free energy change of binding (ΔG) of $-42.26 \text{ KJ mol}^{-1}$ was achieved for the

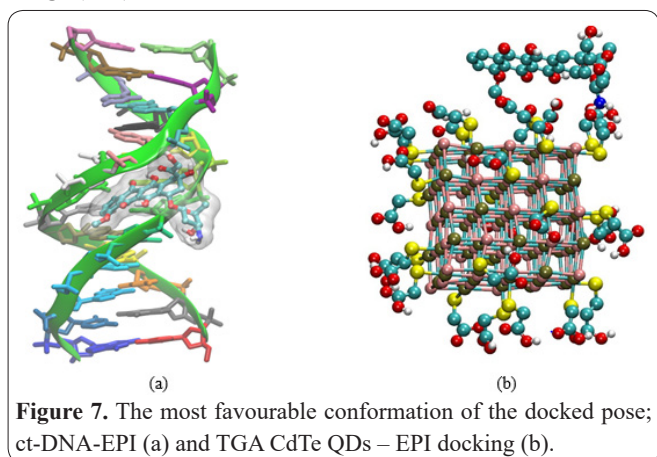


Figure 7. The most favourable conformation of the docked pose; ct-DNA-EPI (a) and TGA CdTe QDs – EPI docking (b).

Table 1. Docking summary of EPI with both ct-DNA and TGA capped CdTe-QDs.

	Cluster -Rank	Run	Lowest Free Energy of Binding (KJ mol^{-1})	Inhibition Constant (K_i)	RMSD from reference structure (Å)
EPI-ct-DNA	1	30	-42.26	118.4 nM	27.66
EPI- TGA CdTe-QDs	1	35	-20.11	42.73 uM	30.800

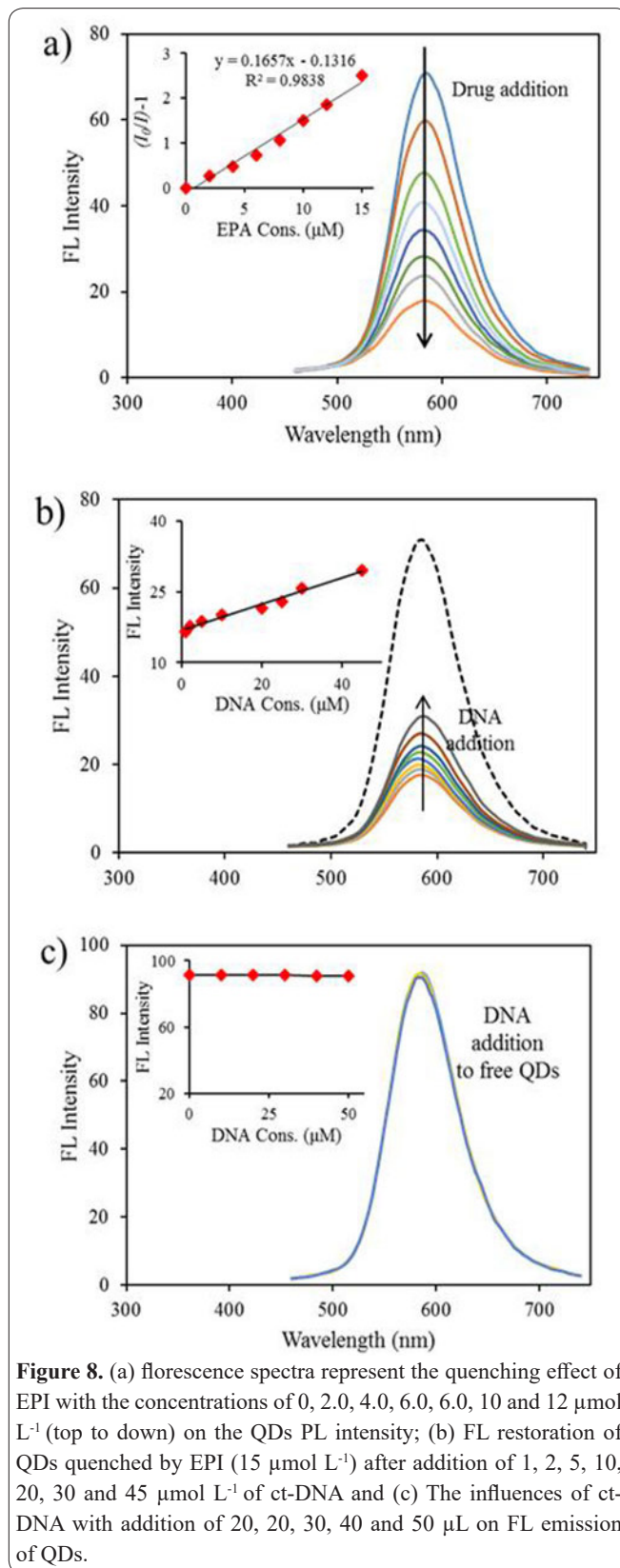


Figure 8. (a) fluorescence spectra represent the quenching effect of EPI with the concentrations of 0, 2.0, 4.0, 6.0, 8.0, 10 and 12 $\mu\text{mol L}^{-1}$ (top to down) on the QDs PL intensity; (b) FL restoration of QDs quenched by EPI ($15 \mu\text{mol L}^{-1}$) after addition of 1, 2, 5, 10, 20, 30 and 45 $\mu\text{mol L}^{-1}$ of ct-DNA and (c) The influences of ct-DNA with addition of 20, 20, 30, 40 and 50 μL on FL emission of QDs.

ct-DNA-EPI complex. From obtained ΔG and the $\Delta G = RT \ln K$ equation the K_b of $2.5 \times 10^7 \text{ M}^{-1}$. As demonstrated by docking and UV-Vis studies the EPI interacts with DNA, so the drug can be adsorbed with DNA. Therefore, ct-DNA should be able to separate the drug

from the surface of investigated CdTe QDs.

FL study and EPI-ct-DNA parameters investigation

For TGA-CdTe QDs solution FL was achieved in 590 nm under excitation at 340 nm. FL spectra of the solution containing a mixed amount of CdTe QDs and EPI are shown in Figure 8 a. Apparently, the fluorescence intensity of CdTe QDs is quenched with the increased EPI concentration. Also, the adequate binding energy for the EPI-QDs obtained from docking proved the FL quenching by the EPI.

The FL intensity of the CdTe QDs/EPI hybrids is then regularly enhanced with the increased ct-DNA concentration (Figure 8 b). By adding the ct-DNA concentration from zero to 45 $\mu\text{mol L}^{-1}$, the FL intensity of CdTe QDs varied less strictly. EPI has a strong quenching effect on fluorescence of QDs, and the addition of DNA will restore the fluorescence of this hybrids. EPI was embedded into ct-DNA with hydrogen bonds having more selectivity rather than QDs.

For further investigation of interactions the K_b of ct-DNA and EPI calculated by the following equation (Eq. 3) (28):

$$I_0 = 1 - k \times \left\{ \frac{-\left(\frac{K_b C_{NP}}{2s} - K_b C_t + 1\right) + \left[\left(\frac{K_b C_{NP}}{2s} - K_b C_t + 1\right)^2 + 4K_b C_t\right]^{1/2}}{2K_b} \right\} \quad \text{Eq. 3}$$

where k , C_{NP} , K_b , s , and C_t belong to the linear regression curve, which on behalf of the connection among I/I_0 and the EPI value represent nucleotide phosphate concentration the K_b , binding site size of EPI with ct-DNA and the total concentration of EPI in the media, respectively.

The value of I/I_0 varied by changing the concentration of nucleotide phosphate (C_{NP}). Thus, using the non-linear fit of Eq. 3 for the EPI - ct-DNA complex, the K_b and s (binding site size) were achieved. The connection of I/I_0 with C_{NP} is shown in Figure 8 b. The obtained K_b was $8.0 \times 10^7 \text{ M}^{-1}$ and the s was 6.45 bp (12.9 bases).

Discussion

The morphological changes of biological macromolecules after blending with the chemical agents characterized using several techniques and approach (29) for more understanding about the nature of this interaction. EPI is one of these chemical agents which as a cancerous drug, the interaction between that and DNA was studied in some paper. By these studies the mode of EPI action in cancer treatment determined. Erdem and Ozsoz studied the interaction of EPI with ct-DNA using electrochemical methods including differential pulse voltammetry and cyclic voltammetry at carbon paste electrode (30). The EPI interaction in this study characterized by spectroscopy, fluorescence study using TGA capped CdTe QDs (31) and MD (32) techniques.

The K_b amount from spectroscopy method was calculated to be $3.00 \times 10^6 \text{ M}^{-1}$. Charak *et al.* were evaluated the EPI and DNA interaction. This study finding was shown the partial transition from B-conformation of DNA to A-conformation which proved the EPI interaction with DNA (33). Nafisi *et al.* in one study achieved the value of $6.58 \times 10^4 \text{ M}^{-1}$, $2.69 \times 10^4 \text{ M}^{-1}$ and

$2.13 \times 10^4 \text{ M}^{-1}$ as a K_b of ethidium bromide, acridine orange, methylene blue, respectively (34). These fluorescent compounds bind to DNA via intercalative mode. The findings (higher EPI-DNA K_b in comparison with fluorescent compounds) were demonstrated the strong intercalation of EPI to the DNA base pair.

Molecular docking approach is an attractive approach to probe the biomolecule-drug interactions. This could be used for different purposes such as the rational drug design and discovery. The other main purpose is the mechanistic study of ligand pose in the binding pocket, which can be performed by placing a small molecule (usually a drug or drug-like compound) into the binding site of the DNA, proteins, enzymes and etc. mainly in an electrostatic interaction mode. For biological macromolecules, the structural behaviour of molecules leads to the variable mode of binding; actually, the molecular 3D structure is an important factor which affects the binding mechanism (35). The most promising conformation of the docked pose in our work exposed that EPI combined with ct-DNA via intercalation mode to the ct-DNA (H-bonding with EPI NH_2 group). Similar results reported for doxorubicin-DNA interaction by docking investigation (36).

Nano-biosensors with so many technique and materials were used for the detection and measurement of several agents in the nanobiotechnology (37). QDs based assay technique has more sensitivity rather than other methods including electrochemical or spectrochemical technique (38). The achieved QDs in this study can exit with a single excitation source. By these advantages, the modified QDs could be used as an alternative of the organic fluorophores in the analytical methods, which needed the excitation light source be tuned into their respective narrow absorption bands (39). Anticancer drugs like EPI and doxorubicin are a good electron acceptor and reduce the fluorescence of QDs. In this condition, the hydrogen bonding and electrostatic attraction caused the gathering of TGA capped CdTe QDs and EPI. K_b obtained from this method is similar to that obtained with docking and spectroscopy studies and similar to other results obtained for anthracycline drugs (40, 41).

The TGA that caps the CdTe QDs firstly enhanced the water-solubility and at the same time caused the negative charge for obtained QDs. EPI has a positive charge in the investigated condition, thus, EPI and TGA-capped CdTe QDs were aggregated with electrostatic force, which quenches the QDs FL and formed the sensor which can detect the concentration of biomaterial that should be content with this kind of drugs. The ct-DNA have negative charge in the investigated condition. This same charge caused the less attraction between QDs and ct-DNA. In the same time, the attraction forces between EPI and DNA caused the interaction of these agents in the presence of QDs.

From the mentioned results it was proved the insertion of the investigated drug into the ct-DNA occur from the planer part. The obtained results with more accuracy are in the agreement with previous results which proved the intercalation of the EPI to DNA.

In the paper, the mode of EPI interaction with ct-DNA investigated by spectroscopic study, fluorescent QDs, and MD technique. The K_b obtained from docking, spectroscopy and FL investigation. The result achieved

by Docking is in agreement with the experimental results. From the docking simulation with the energetically optimized conformation, it was demonstrated that EPI intercalated to the ct-DNA and is located within A–T regions in comparison with G–C pairs by the ΔG of $-42.26 \text{ KJ mol}^{-1}$ for the DNA-EPI complex. FL studies show that absorbing of EPI on TGA-CdTe QDs, quench the FL. In the same time, with the adding of a biological agent, ct-DNA was associated with EPI, and EPI will be separated from the surface of TGA-CdTe QDs, leading to the fluorescence recovery. The UV-Vis and MD results of ct-DNA and EPI demonstrated that the reaction between ct-DNA and EPI is superior over the reaction between TGA-capped CdTe QDs and EPI. By K_b investigation in this works the obtained results from both docking and FL study is more similar to each other which proved the suit of FL methods rather than spectroscopic study.

Acknowledgements

This work was performed in the partial fulfillment of the requirements (93525) from Kermanshah University of Medical Sciences, Kermanshah, Iran.

References

1. Brockmann H. Anthracyclines and anthracyclines. (Rhodomycinone, pyromycinone and their glycosides). *Fortschritte der Chemie organischer Naturstoffe= Progress in the chemistry of organic natural products Progres dans la chimie des substances organiques naturelles* 1963; 21: 121.
2. Gabbay E, Grier D, Fingerle R et al. Interaction specificity of the anthracyclines with deoxyribonucleic acid. *Biochemistry-US* 1976; 15(10): 2062-2070.
3. Gu X, Jia S, Wei W, Zhang W-H. Neoadjuvant chemotherapy of breast cancer with pirarubicin versus epirubicin in combination with cyclophosphamide and docetaxel. *Tumor Biol* 2015; 36(7): 5529-5535.
4. Tariq M, Alam MA, Singh AT, Iqbal Z, Panda AK, Talegaonkar S. Biodegradable polymeric nanoparticles for oral delivery of epirubicin: in vitro, ex vivo, and in vivo investigations. *Colloid Surface B* 2015; 128: 448-456.
5. Kumar R, Lown JW. Design, synthesis and in vitro cytotoxic studies of novel bis-pyrrolo [2, 1][1, 4] benzodiazepine-pyrrole and imidazole polyamide conjugates. *Eur J Med Chem* 2005; 40(7): 641-654.
6. Gu X, Jia S, Wei W, Zhang W-H. Neoadjuvant chemotherapy of breast cancer with pirarubicin versus epirubicin in combination with cyclophosphamide and docetaxel. *Tumor Biol* 2015: 1-7.
7. Chen H, Gao J, Lu Y et al. Preparation and characterization of PE38KDEL-loaded anti-HER2 nanoparticles for targeted cancer therapy. *J Control Release* 2008; 128(3): 209-216.
8. Pakravan P, Masoudian S. Study on the Interaction between isatin- β -thiosemicarbazone and calf thymus DNA by spectroscopic techniques. *Iran J Pharm Res* 2015; 14(1): 111.
9. Li H, Bu X, Lu J, Xu C, Wang X, Yang X. Interaction study of ciprofloxacin with human telomeric DNA by spectroscopy and molecular docking. *Spectrochim Acta A* 2013; 107: 227-234.
10. Lauria A, Tutone M, Almerico AM. Design of new DNA-interactive agents by molecular docking and QSPR approach. *Arkivoc* 2010; 11: 13-27.
11. Pathak S, Choi S-K, Arnheim N, Thompson ME. Hydroxylated quantum dots as luminescent probes for in situ hybridization. *J Am Chem Soc* 2001; 123(17): 4103-4104.

12. Koneswaran M, Narayanaswamy R. Retraction Note to: CdS/ZnS core-shell quantum dots capped with mercaptoacetic acid as fluorescent probes for Hg (II) ions. *Microchim Acta* 2016; 183(4): 1519-1519.
13. Miao Y, Zhang Z, Gong Y, Yan G. Phosphorescent quantum dots/doxorubicin nano hybrids based on photoinduced electron transfer for detection of DNA. *Biosens Bioelectron* 2014; 59: 300-306.
14. Raymo FM, Yildiz I. Luminescent chemosensors based on semiconductor quantum dots. *Phys Chem Chem Phys* 2007; 9(17): 2036-2043.
15. Medintz IL, Clapp AR, Mattoussi H, Goldman ER, Fisher B, Mauro JM. Self-assembled nanoscale biosensors based on quantum dot FRET donors. *Nat Mater* 2003; 2(9): 630-638.
16. Shi L, Rosenzweig N, Rosenzweig Z. Luminescent quantum dots fluorescence resonance energy transfer-based probes for enzymatic activity and enzyme inhibitors. *Anal Chem* 2007; 79(1): 208-214.
17. Jepsen ML, Harmsen C, Godbole AA, Nagaraja V, Knudsen BR, Ho Y-P. Specific detection of the cleavage activity of mycobacterial enzymes using a quantum dot based DNA nanosensor. *Nanoscale* 2016; 8(1): 358-364.
18. Zhang J, Tu L, Zhao S et al. Fluorescent gold nanoclusters based photoelectrochemical sensors for detection of H₂O₂ and glucose. *Biosens Bioelectron* 2015; 67: 296-302.
19. Bozdemir OA, Sozmen F, Buyukcakir O, Guliyev R, Cakmak Y, Akkaya EU. Reaction-based sensing of fluoride ions using built-in triggers for intramolecular charge transfer and photoinduced electron transfer. *Org Lett* 2010; 12(7): 1400-1403.
20. Zhang L, Zhu J, Guo S, Li T, Li J, Wang E. Photoinduced electron transfer of DNA/Ag nanoclusters modulated by G-quadruplex/hemin complex for the construction of versatile biosensors. *J Am Chem Soc* 2013; 135(7): 2403-2406.
21. Yildiz I, Tomasulo M, Raymo FM. A mechanism to signal receptor-substrate interactions with luminescent quantum dots. *Proc Natl Acad Sci* 2006; 103(31): 11457-11460.
22. Bera S, Singh SB, Ray SK. Green route synthesis of high quality CdSe quantum dots for applications in light emitting devices. *J Solid State Chem* 2012; 189: 75-79.
23. Barati A, Shamsipur M, Abdollahi H. Hybrid of non-selective quantum dots for simultaneous determination of TNT and 4-nitrophenol using multivariate chemometrics methods. *Anal Methods* 2014; 6(16): 6577-6584.
24. Kashanian S, Khodaei MM, Pakravan P. Spectroscopic studies on the interaction of isatin with calf thymus DNA. *DNA Cell Biol* 2010; 29(10): 639-646.
25. Qais FA, Abdullah KM, Alam MM, Naseem I, Ahmad I. Interaction of capsaicin with calf thymus DNA: A multi-spectroscopic and molecular modelling study. *Int J Biol Macromol* 2017; 97: 392-402.
26. Liu XW, Li J, Deng H, Zheng KC, Mao ZW, Ji LN. Experimental and DFT studies on the DNA-binding trend and spectral properties of complexes [Ru (bpy)₂L]²⁺ (L= dmdpq, dpq, and dcdpq). *Inorg Chim Acta* 2005; 358(12): 3311-3319.
27. Wei W, Gao SG, Shi NN. Study on the interaction between gatifloxacin mesylate and salmon sperm DNA by fluorescence method. *J Chin Chem Soc-TAIP* 2006; 53(3): 721-726.
28. Yuan J, Guo W, Yang X, Wang E. Anticancer drug-DNA interactions measured using a photoinduced electron-transfer mechanism based on luminescent quantum dots. *Anal Chem* 2008; 81(1): 362-368.
29. Kashanian S, Khodaei MM, Pakravan P, Adibi H. Molecular aspects on the interaction of isatin-3-isonicotinylhydrazone to deoxyribonucleic acid: model for intercalative drug-DNA binding. *Mol Biol Rep* 2012; 39(4): 3853-3861.
30. Erdem A, Ozsoz M. Interaction of the anticancer drug epirubicin

with DNA. *Anal Chim Acta* 2001; 437(1): 107-114.

31. Apilux A, Siangproh W, Insin N, Chailapakul O, Prachayasittikul V. Paper-based thioglycolic acid (TGA)-capped CdTe QD device for rapid screening of organophosphorus and carbamate insecticides. *Anal Methods* 2017; 9(3) 519-527.

32. Shahabadi N, Moradi F, Fili S, Shahlaei M. Synthesis, characterization and comparative DNA interaction studies of new copper (II) and nickel (II) complexes containing mesalamine drug using molecular modeling and multispectroscopic methods. *J Coord Chem* 2015; 68(20): 3667-3684.

33. Charak S, Jangir DK, Tyagi G, Mehrotra R. Interaction studies of Epirubicin with DNA using spectroscopic techniques. *Journal of Molecular Structure* 2011; 1000(1-3): 150-154.

34. Nafisi S, Saboury AA, Keramat N, Neault J-F, Tajmir-Riahi H-A. Stability and structural features of DNA intercalation with ethidium bromide, acridine orange and methylene blue. *J Mol Struct* 2007; 827(1): 35-43.

35. Arjmand F, Parveen S, Afzal M, Toupet L, Hadda TB. Molecular drug design, synthesis and crystal structure determination of Cu II-Sn IV heterobimetallic core: DNA binding and cleavage studies.

Eur J Med Chem 2012; 49: 141-150.

36. Agudelo D, Bourassa P, Bérubé G, Tajmir-Riahi H. Review on the binding of anticancer drug doxorubicin with DNA and tRNA: Structural models and antitumor activity. *J Photoch Photobio B* 2016; 158: 274-279.

37. Moradi S, Khaledian S, Abdoli M, Shahlaei M, Kahrizi D. Nanobiosensors in cellular and molecular biology. *Cell Mol Biol* 2018; 64 (5): 85-90.

38. Huang X, Zhan S, Xu H, Meng X, Xiong Y, Chen X. Ultrasensitive fluorescence immunoassay for detection of ochratoxin A using catalase-mediated fluorescence quenching of CdTe QDs. *Nanoscale* 2016; 8(17): 9390-9397.

39. Hohng S, Ha T. Single-molecule quantum-dot fluorescence resonance energy transfer. *ChemPhysChem* 2005; 6(5): 956-960.

40. Byrn SR, Dolch GD. Analysis of binding of daunorubicin and doxorubicin to DNA using computerized curve-fitting procedures. *J Pharm Sci* 1978; 67(5): 688-693.

41. Ibrahim MS. Voltammetric studies of the interaction of nogalamycin antitumor drug with DNA. *Anal Chim Acta* 2001; 443(1): 63-72.